Received: 2 December 2020 | Revised: 19 January 2021 | Accepted: 26 January 2021

DOI: 10.1111/cas.14832

ORIGINAL ARTICLE

Cancer Science WILEY

Forecasting sensitive targets of the kynurenine pathway in pancreatic adenocarcinoma using mathematical modeling

Murad Alahdal[1,2,3] | Deshun Sun[1] | Li Duan[1] | Hongwei Ouyang[2] | Manyi Wang[1] | Jianyi Xiong[1] | Daping Wang[1,4]

[1]Shenzhen Key Laboratory of Tissue Engineering, Shenzhen Laboratory of Digital Orthopedic Engineering, Guangdong Provincial Research Center for Artificial Intelligence and Digital Orthopedic Technology, Shenzhen Second People's Hospital (The First Hospital Affiliated to Shenzhen University, Health Science Center), Shenzhen, China

[2]Dr. Li Dak Sum & Yip Yio Chin Center for Stem Cells and Regenerative Medicine, Zhejiang University School of Medicine, Hangzhou, China

[3]Department of Medical Laboratories, Faculty of Medicine, Hodeidah University, Al Hudaydah, Yemen

[4]Department of Biomedical Engineering, Southern University of Science and Technology, Shenzhen, China

Correspondence
Daping Wang and Jianyi Xiong, Shenzhen Second People's Hospital (The First Hospital Affiliated to Shenzhen University, Health Science Center), Shenzhen 518035, China.
Emails: wangdp@mail.sustech.edu.cn; jianyixiong@126.com

Funding information
National Natural Science Foundation of China, Grant/Award Number: 81972116, 81972085 and 81772394; Key Program of Natural Science Foundation of Guangdong Province, Grant/Award Number: 2018B0303110003; Shenzhen Peacock Project, Grant/Award Number: KQTD20170331100838136; Shenzhen Science and Technology Projects, Grant/Award Number: JCYJ20170817172023838, JCYJ20170306092215436, JCYJ20170412150609690, JCYJ20170413161649437 and JCYJ20170413161800287

Abstract

In this study, a new mathematical model was established and validated to forecast and define sensitive targets in the kynurenine pathway (Kynp) in pancreatic adenocarcinoma (PDAC). Using the Panc-1 cell line, genetic profiles of Kynp molecules were tested. qPCR data were implemented in the algorithm programming (*fmincon* and *lsqnonlin* function) to estimate 35 parameters of Kynp variables by Matlab 2017b. All tested parameters were defined as non-negative and bounded. Then, based on experimental data, the function of the *fmincon* equation was employed to estimate the approximate range of each parameter. These calculations were confirmed by qPCR and Western blot. The correlation coefficient (*R*) between model simulation and experimental data (72 hours, in intervals of 6 hours) of every variable was >0.988. The analysis of reliability and predictive accuracy depending on qPCR and Western blot data showed high predictive accuracy of the model; *R* was >0.988. Using the model calculations, *kynurenine* (*x3*, *a6*), *GPR35* (*x4*, *a8*), *NF-kβp105* (*x7*, *a16*), and *NF-kβp65* (*x8*, *a18*) were recognized as sensitive targets in the Kynp. These predicted targets were confirmed by testing gene and protein expression responses. Therefore, this study provides new interdisciplinary evidence for Kynp-sensitive targets in the treatment of PDAC.

KEYWORDS

kynurenine pathway, mathematical modeling, Matlab 2017b, pancreatic adenocarcinoma, sensitive targets

Alahdal, Sun and Duan are equally cooperated in this study.

1 | INTRODUCTION

Pancreatic adenocarcinoma (PDAC) is the 12th most common cancer worldwide.[1] According to The Surveillance, Epidemiology, and End Result program database reports, the 5-year survival of PDAC patients is around 7.7% with very low improvement.[1] Over 82% of diagnosed patients are at risk of death within a few months because warning signs of PDAC are often not noticeable until the disease has already metastasized to other organs of the body. Statistics alarm that PDAC may become the second leading cause of death among all cancers by 2020.[2] The increase in mortality is due to the lack of effective therapeutic options. The kynurenine pathway (Kynp) plays a significant role in enhancing PDAC growth, immune escape, and immunotolerance.[3,4] Plasma levels of kynurenine, kynurenic acid, and quinolinic acid were found significantly higher in PDAC patients, and the level of tryptophan (the substrate of kynurenine) was very low, suggesting high activity of the Kynp in PDAC.[3] Further, Kynp inhibition showed a promising clinical significance among pancreatic cancer patients (NCT02077881, NCT03414229, NCT03432676). The Kynp activates a variety of signaling molecules in cancer cells.[5] It mainly activates G protein–coupled receptor 35 (GPR35) in the PDAC cell that essentially enhances oncogenic signaling and tumorigenesis progression.[6] GPR35 has the potential to stimulate β-catenin activity in colon, breast, and pancreatic cancers.[7-9] In the PDAC cell, β-catenin induces IκB kinase β (IKK-β) and nuclear factor kappa B (NF-κβ) expression.[10,11] NF-κβ p65[12] and interleukin 6 (IL-6)[13] are consecutive molecules of NF-κβ in the case of Kynp activity. Transforming growth factor beta 1 (TGF-β1) has been reported as an essential biomarker of the Kynp in PDAC.[14-17] Therefore, we have delineated the Kynp in PDAC according to the previous literature mentioned above. However, the most sensitive molecules of the Kynp in PDAC have not been defined yet. The exploration of Kynp-sensitive molecules will substantially contribute to exploring new targets in the treatment of PDAC.

Because the intricacies of sensitive target determination in the whole pathway are challenging, mathematical modelling was established to make the biological changes of Kynp molecules become more quantitative. Different kinds of mathematical models have been established to understand the corresponding mechanism for some diseases.[18,19] Hence, the mathematical model has the potential to provide a reasonable explanation for the activity of Kynp molecules in PDAC. In this study, we established a mathematical model to determine sensitive and insensitive molecules of the Kynp in PDAC accurately, which can be considered as critical targets for treating PDAC.

2 | MATERIALS AND METHODS

2.1 | Cell culture and Kynp stimulation

Human PDAC cell line (Panc-1 ATCC® CRL-1469™) was purchased from the ATCC. Panc-1 cells were plated in Dulbecco's Modified Eagle Medium (DMEM) basic (1×) (Gibco). DMEM was supplemented by 10% fetal bovine serum (FBS) (Gibco) and 1% penicillin/streptomycin (ATLANTA Biologicals). Next, cells were collected and washed twice with phosphate-buffered saline (PBS). Then, 1×10^6 cells/well were cultured in a 48-well plastic plate (Corning Costar). Thereafter, cell culture medium was supplemented by 1 μg/mL L-Tryptophan (Sigma-Aldrich) and incubated for 72 hours. A total of 20 ng/mL of human purified recombinant indoleamine 2,3 dioxygenase1 (hIDO1) (Prospec) was added every 6 hours to stimulate the Kynp in the tumor cells. This culture system was duplicated and repeated three times.

2.2 | Gene expression profiling

Culture medium was aspirated carefully into numbered sterile plastic tubes and kept in the refrigerator at 4°C for further analysis. Cells were detached by trypsin and washed with sterile PBS twice. Then, total RNA of tumor cells was extracted by TRIzol standard protocol.[20] Next, the RNA was reverse transcribed to cDNA according to kit instructions (Takara). Later, the template cDNA was used with the primers of the following genes: *kynurenine 3-monooxygenase*, *GPR35*, *β-catenin*, *IKK-β*, *NF-κβp105*, *ANK*, *RelA*, *IL-6*, and *TGF-β1*. Forward and reverse primers listed in Table S1 were designed using NCBI gene IDs and Primer Bank website (https://pga.mgh.harvard.edu/primerbank/). Relative mRNA expression was calculated according to $2^{-\Delta\Delta ct}$.

2.3 | Protein expression levels

2.3.1 | Enzyme-Linked Immunosorbent Assay (ELISA)

To validate our model at protein expression level, four molecules of the Kynp have been tested at twelve time points using ELISA kits

FIGURE 1 Using qPCR the gene relative expression of Kynp parameters in Panc-1 was analyzed from 6 h to 72 h. A, Expression level of kynurenine (x3). B, Relative expression level of GPR35 (x4). C, Gene relative expression of β-catenin (x5). D, Gene relative expression of IKKβ (x6). E, Gene relative expression of NF-κβp105 (x7). F, Gene relative expression of ANK (x9). G, Gene relative expression of RelA (x10). H, Gene relative expression of IL-6 (x11). I, Gene relative expression of TGF-β (x12). Then, the mathematical model was established by parameter estimation at the mRNA expression level. J, K, Q, Simulation trends of tryptophan, IDO1, and NF-κβp65 are presented as blue line from 0 h to 72 h based on the established model. L-P, R-U Validation of Kyn, GPR35, β-catenin, IKK-β, NF-κβp105, ANK, RelA, IL-6, and TGF-β1 was performed by plotting the experimental findings, shown as red line, and model simulation, shown as blue line 0 h to 72 h (error bars, mean ± SD)

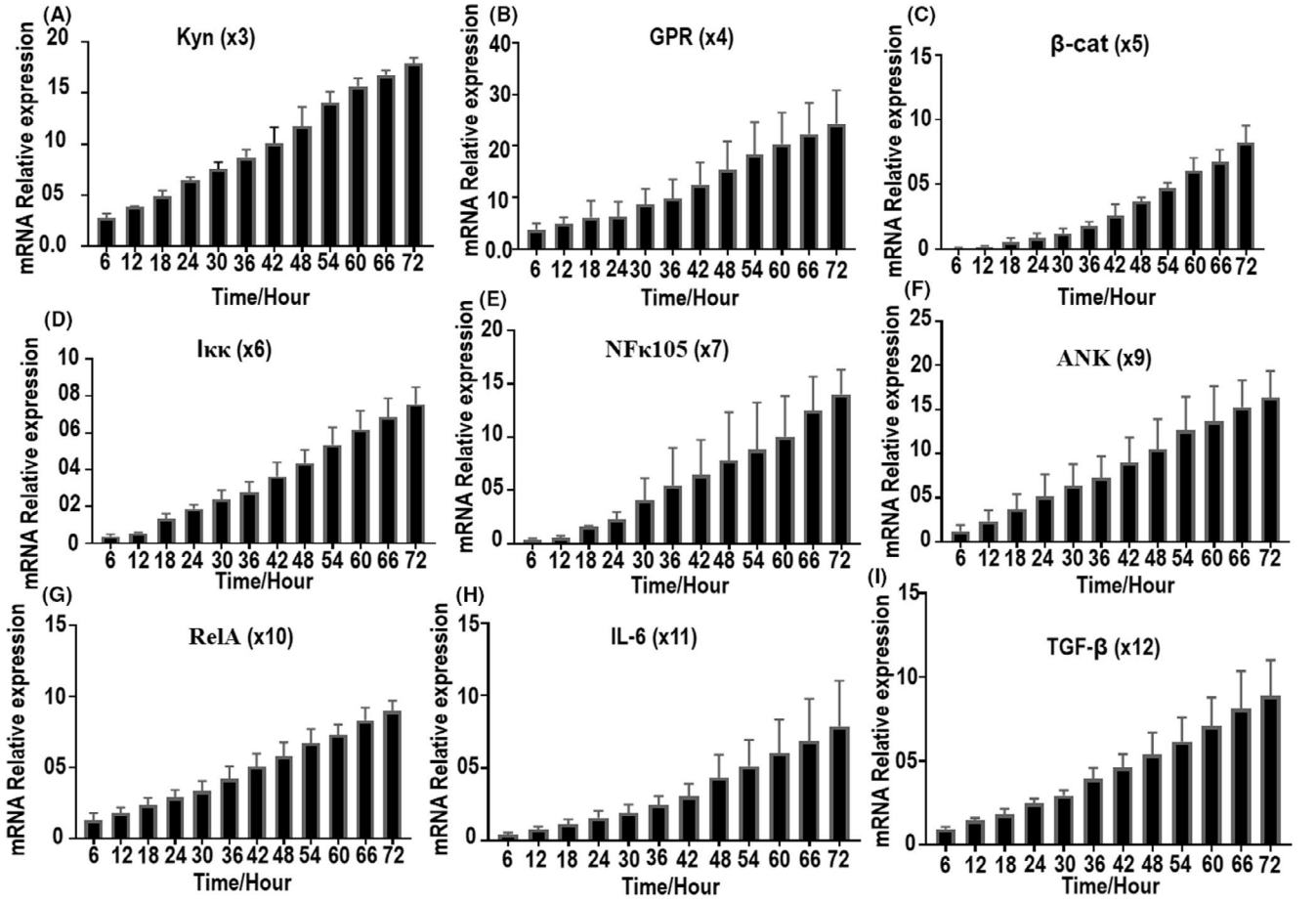
(A)
Kyn (x3)
mRNA Relative expression
Time/Hour
(B)
GPR (x4)
mRNA Relative expression
Time/Hour
(C)
β-cat (x5)
mRNA Relative expression
Time/Hour
(D)
Iκκ (x6)
mRNA Relative expression
Time/Hour
(E)
NFκ105 (x7)
mRNA Relative expression
Time/Hour
(F)
ANK (x9)
mRNA Relative expression
Time/Hour
(G)
RelA (x10)
mRNA Relative expression
Time/Hour
(H)
IL-6 (x11)
mRNA Relative expression
Time/Hour
(I)
TGF-β (x12)
mRNA Relative expression
Time/Hour

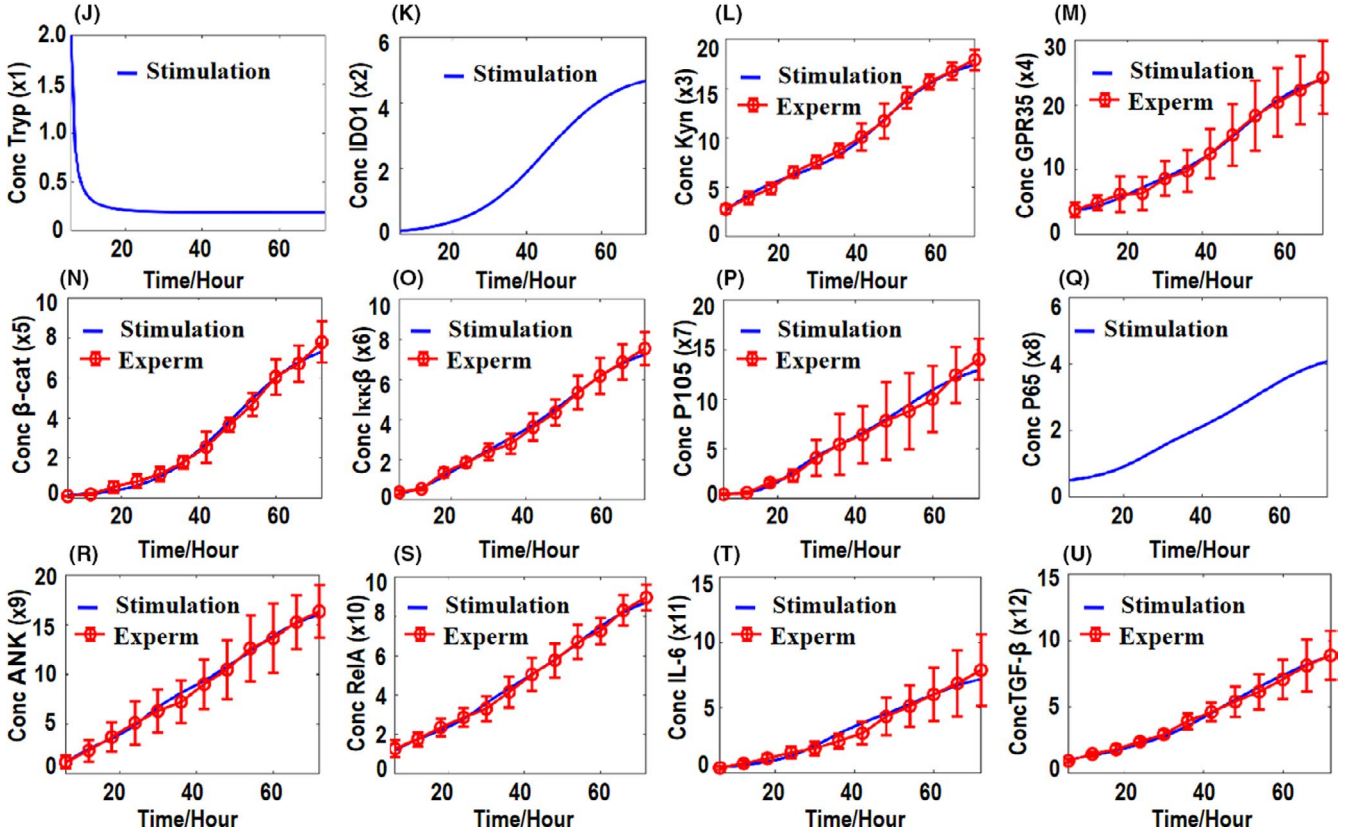
(J)
Conc Tryp (x1)
Stimulation
Time/Hour
(K)
Conc IDO1 (x2)
Stimulation
Time/Hour
(L)
Conc Kyn (x3)
Stimulation
Experm
Time/Hour
(M)
Conc GPR35 (x4)
Stimulation
Experm
Time/Hour
(N)
Conc β-cat (x5)
Stimulation
Experm
Time/Hour
(O)
Conc Iκκβ (x6)
Stimulation
Experm
Time/Hour
(P)
Conc P105 (x7)
Stimulation
Experm
Time/Hour
(Q)
Conc P65 (x8)
Stimulation
Time/Hour
(R)
Conc ANK (x9)
Stimulation
Experm
Time/Hour
(S)
Conc RelA (x10)
Stimulation
Experm
Time/Hour
(T)
Conc IL-6 (x11)
Stimulation
Experm
Time/Hour
(U)
ConcTGF-β (x12)
Stimulation
Experm
Time/Hour

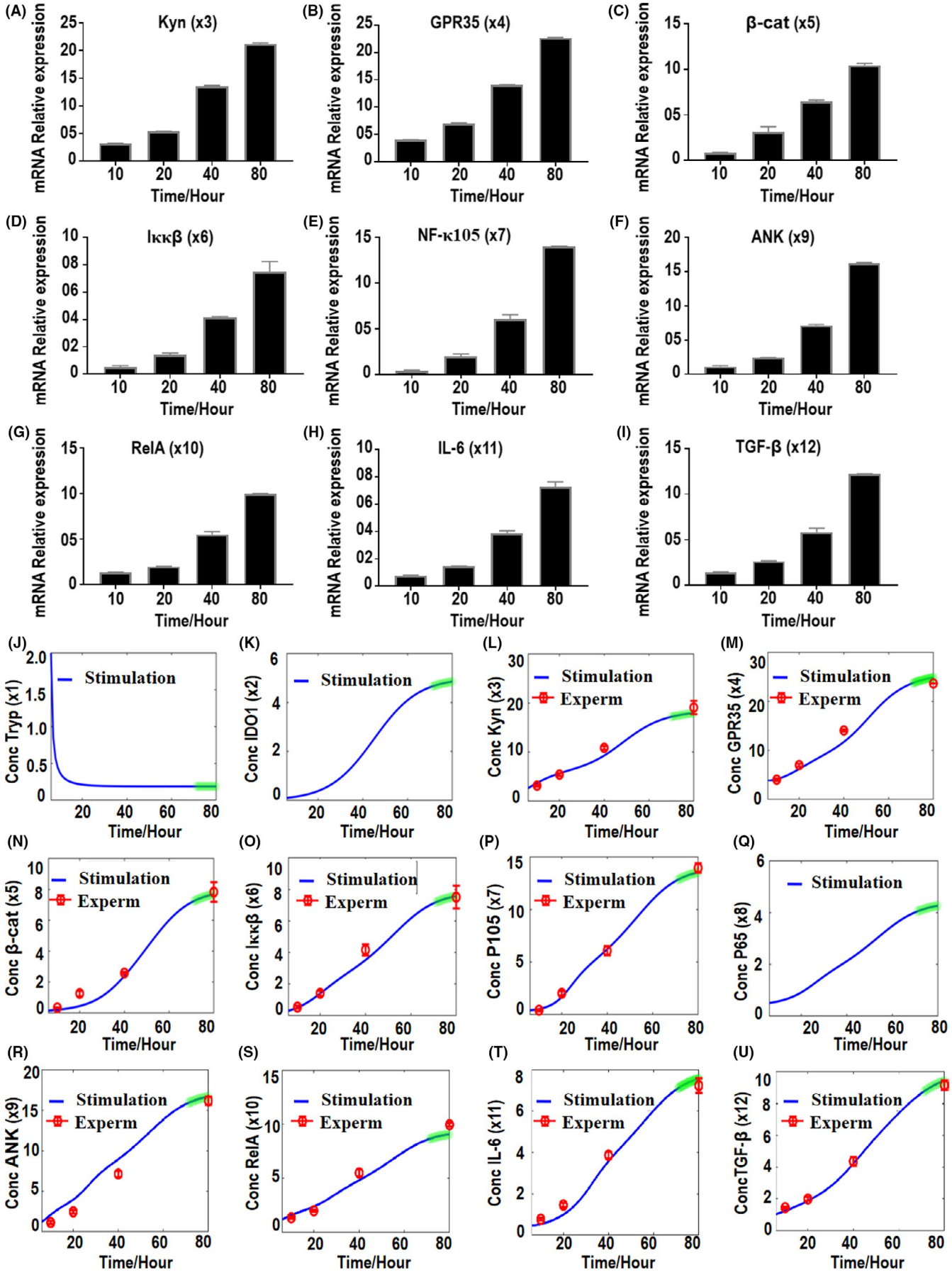
(A)
Kyn (x3)
mRNA Relative expression
Time/Hour
(B)
GPR35 (x4)
mRNA Relative expression
Time/Hour
(C)
β-cat (x5)
mRNA Relative expression
Time/Hour
(D)
Ikkβ (x6)
mRNA Relative expression
Time/Hour
(E)
NF-κ105 (x7)
mRNA Relative expression
Time/Hour
(F)
ANK (x9)
mRNA Relative expression
Time/Hour
(G)
RelA (x10)
mRNA Relative expression
Time/Hour
(H)
IL-6 (x11)
mRNA Relative expression
Time/Hour
(I)
TGF-β (x12)
mRNA Relative expression
Time/Hour
(J)
Conc Tryp (x1)
Stimulation
Time/Hour
(K)
Conc IDO1 (x2)
Stimulation
Time/Hour
(L)
Conc Kyn (x3)
Stimulation
Experm
Time/Hour
(M)
Conc GPR35 (x4)
Stimulation
Experm
Time/Hour
(N)
Conc β-cat (x5)
Stimulation
Experm
Time/Hour
(O)
Conc Ikkβ (x6)
Stimulation
Experm
Time/Hour
(P)
Conc P105 (x7)
Stimulation
Experm
Time/Hour
(Q)
Conc P65 (x8)
Stimulation
Time/Hour
(R)
Conc ANK (x9)
Stimulation
Experm
Time/Hour
(S)
Conc RelA (x10)
Stimulation
Experm
Time/Hour
(T)
Conc IL-6 (x11)
Stimulation
Experm
Time/Hour
(U)
ConcTGF-β (x12)
Stimulation
Experm
Time/Hour

FIGURE 2 qPCR analysis of the accuracy and predictability of the Kynp math model was performed at four time points from 10 h to 40 h for an accuracy test and from 72 h to 80 h for the predictability assessment. A-I, Gene relative expression of the Kynp variables at 10 h, 20 h, 40 h, and 80 h. Then, the verification of the established mathematical model was performed based on the mRNA expression level. J, K, Q, Simulated trends of Tryptophan, IDO1, and NF-κβp65 are presented as blue line from 0 h to 80 h based on the established model. L-P, R-U, Accuracy test of Kyn, GPR35, β-catenin, IKK-β, NF-κβp105, ANK, RelA, IL-6, and TGF-β1 was presented as red points at time points 10 h, 20 h, 40 h. Consequently, the predictability was presented by the red points at time points 80 h. Model simulations were correspondingly shown as blue and green line, respectively

from 6 hours to 72 hours. Supernatant was aspirated into sterile tubes and then saved in the refrigerator at 4°C. Later, the protein expression levels of kynurenine (Biocompare), β-catenin (BioVision), NF-κβp65 (Path-ScanR), and TGF-β1 (Multi-Sciences) in the culture supernatants were tested according to the kit's manufacturers' instructions.

2.3.2 | Western blot

In terms of model verification, tumor cells were cultured by the same protocol as described above. Briefly, eight time points were selected for testing protein expression (6 hours, 10 hours, 20 hours, 30 hours, 40 hours, 50 hours, 60 hours, and 80 hours), and then cells were collected and washed twice with PBS. Total protein was extracted by radioimmunoprecipitation assay (RIPA) buffer mixed with 1% phenyl methyl sulfonyl fluoride (PMSF) proteinase inhibitor for 30 minutes on ice (vortex interval: 10 minutes) and then centrifuged for 10 minutes at 106 *g*/min. The supernatant was transferred into 1-mL Eppendorf tubes. Total protein samples were loaded by protein-loading buffer at 100°C for 10 minutes. Next, 50 ng/mL of total protein was run on the gel and then transblotted on the PVDF membrane. Thereafter, goat milk fixation was performed. Then, protein bands were visualized by human anti-GPR35 antibody (NOVUSBIO), human anti-β-catenin antibody (Proteintech), human anti-NF-κβp105 antibody (Cell Signaling Technology), and human anti-TGF-β1 antibody (Abcam). Then, they were incubated with anti-rabbit IgG for 2 hours, washed three time with Tris-buffered saline buffer, and then were visualized by Odyssey FC (LICOR).

2.4 | Mathematical model establishment

A mathematical model for the Kynp in PDAC cells was proposed based on previous literature that mention the molecules which actively participate in the Kynp in different tumor types. These molecules were all tested in the Panc-1 cell line. According to the gene expression of these molecules, a mathematical model was proposed as the following equation system considering concentration and time of expression for every variable:

$$\begin{cases} \dot{x}_1(t) = (a_1 - b_1 x_1(t))x_1(t), \\ \dot{x}_2(t) = (a_2 - b_2 x_2(t))x_2(t), \\ \dot{x}_3(t) = (a_3 - b_3 x_3(t))x_3(t) + a_4 x_1(t)x_2(t)x_3(t), \\ \dot{x}_4(t) = (a_5 - b_4 x_4(t)) + a_6 x_3(t)x_4(t), \\ \dot{x}_5(t) = a_7 + a_8 x_4(t)x_5(t) - b_5 x_5(t), \\ \dot{x}_6(t) = a_9 + a_{10} x_5(t)x_6(t) - b_6 x_6(t), \\ \dot{x}_7(t) = (a_{11} - b_7 x_7(t))x_7(t) + a_{12} x_6(t)x_7(t), \\ \dot{x}_8(t) = (a_{13} + a_{14} x_6(t)x_8(t))x_8(t) - b_8 x_8(t), \\ \dot{x}_9(t) = a_{15} + a_{16} x_7(t)x_9(t) - b_9 x_9(t), \\ \dot{x}_{10}(t) = a_{17} + a_{18} x_8(t)x_{10}(t) - b_{10} x_{10}(t), \\ \dot{x}_{11}(t) = (a_{19} - b_{11} x_{11}(t))x_{11}(t) + a_{20} x_9(t)x_{11}(t) + a_{21} x_{10}(t)x_{11}(t), \\ \dot{x}_{12}(t) = (a_{22} - b_{12} x_{12}(t))x_{12}(t) + a_{23} x_{11}(t)x_{12}(t). \end{cases} \quad (1)$$

where $x_1(t), x_2(t), x_3(t), x_4(t), x_5(t), x_6(t), x_7(t), x_8(t), x_9(t), x_{10}(t), x_{11}(t)$, and $x_{12}(t)$ represent the relative expression of Tryptophan, IDO1, Kyn, GPR35, β-catenin, IKK-β, NF-κβp105, NF-κβp65, ANK, RelA, IL-6, and TGF-β1, respectively. Parameters ($a_1, a_2, a_3, a_5, a_7, a_9, a_{11}, a_{13}, a_{15}, a_{17}, a_{19}, a_{22}, b_1, b_2, b_3, b_4, b_5, b_6, b_7, b_8, b_9, b_{10}, b_{11}, b_{12}$) represent production and degradation rate of Tryptophan, IDO1, Kyn, GPR35, β-catenin, IKK-β, NF-κβp105, NF-κβp65, ANK, RelA, IL-6, and TGF-β1, respectively. a_4 denotes the activation rate from Tryptophan and IDO1 to Kyn. a_6 denotes the activation rate from Kyn to GPR35. a_8 denotes the activation rate from GPR35 to β-catenin. a_{10} denotes the activation rate from β-catenin to IKK-β. a_{12} denotes the activation rate from IKK-β to NF-κβp105. a_{14} denotes the activation rate from IKK-β to NF-κβp65. a_{16} denotes the activation rate from NF-κβp105 to ANK. a_{18} denotes the activation rate from NF-κβp65 to RelA. a_{20} and a_{21} denote the activation rate from ANK and RelA to IL-6, respectively. a_{23} denotes the activation rate from IL-6 to TGF-β1.

2.4.1 | The estimation of model parameters

In order to get the value of the parameters in Equation (1) based on relative mRNA expression levels, an algorithm (*fmincon* and *lsqnonlin* function) was programmed to estimate the 35 parameters by Matlab 2017b. In this study, all the parameters were defined to be non-negative and bounded because each parameter has its own biological

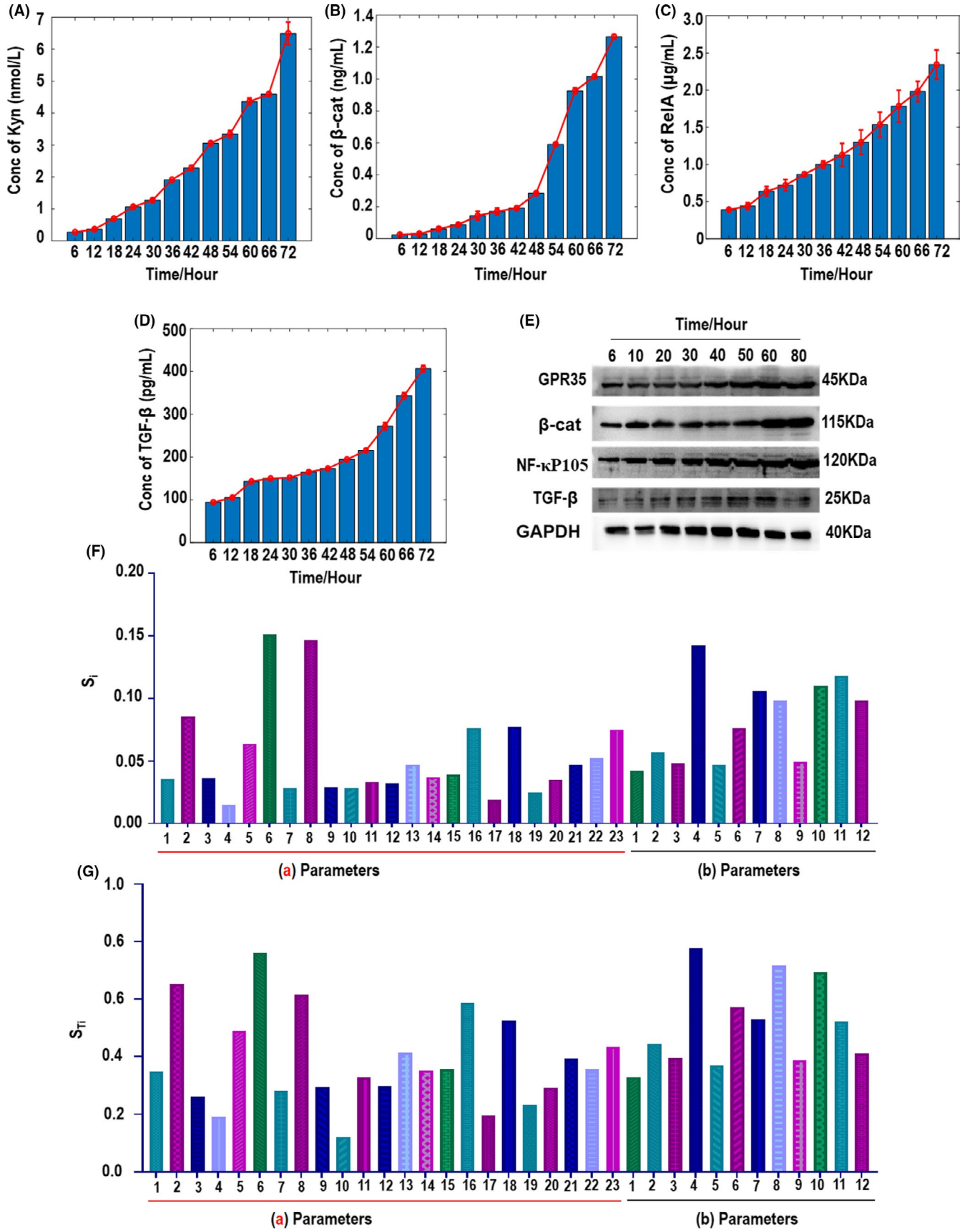

FIGURE 3 Mathematical model verification based on the protein expression level. A-D, ELISA results showed increased protein expression levels of kynurenine, β-catenin, NF-kβp65, and TGF-β1 from 6 h to 72 h. E, Western blot represents protein expression levels of GPR35, β-catenin, NF-kβp105, and TGF-β1 from 6 h to 80 h. Next, the sensitivity analysis was performed using numerical computation. F, The first order sensitive indexes (S_i) of 35 parameters. G, The total sensitive indexes (S_{Ti}) of 35 parameters calculated by extended Fourier amplitude sensitivity test (EFAST)

TABLE 1 The results of sensitivity analysis presenting all parameters

Parameter	a_1	a_2	a_3	a_4	a_5	a_6
S_i	0.0355	0.0854	0.0364	0.0149	0.0636	0.1514
S_{Ti}	0.3487	**0.6516**	*0.2603*	*0.1909*	0.4887	**0.7622**
Parameter	a_7	a_8	a_9	a_{10}	a_{11}	a_{12}
S_i	0.0286	0.1465	0.0291	0.0286	0.0333	0.0317
S_{Ti}	*0.2803*	**0.6172**	*0.2944*	*0.1217*	0.3292	*0.2984*
Parameter	a_{13}	a_{14}	a_{15}	a_{16}	a_{17}	a_{18}
S_i	0.0474	0.0368	0.0392	0.0764	0.0188	0.0772
S_{Ti}	0.4130	0.3524	0.3568	**0.5872**	*0.1953*	**0.5260**
Parameter	a_{19}	a_{20}	a_{21}	a_{22}	a_{23}	b_1
S_i	0.0249	0.0352	0.0469	0.0524	0.0749	0.0424
S_{Ti}	*0.2324*	*0.2907*	0.3934	0.3573	0.4360	0.3276
Parameter	b_2	b_3	b_4	b_5	b_6	b_7
S_i	0.0570	0.0483	0.1424	0.0472	0.0761	0.1063
S_{Ti}	0.4441	0.3952	**0.7760**	0.3701	**0.5709**	**0.5315**
Parameter	b_8	b_9	b_{10}	b_{11}	b_{12}	b_8
S_i	0.0982	0.0492	0.1102	0.1176	0.0978	0.0982
S_{Ti}	**0.7178**	0.3879	**0.6948**	**0.5240**	0.4105	**0.7178**

Bold values denote sensitive parameters; italic values denote insensitive parameters

significance. Secondly, based on experimental data, the *fmincon* function was employed to estimate the approximate range of each parameter. The estimated parameters by the *fmincon* function were regarded as the initial values. Thereafter, further estimation was performed using the *lsqnonlin* function to achieve the best fitting effect between the simulation curve and the experimental data curve.

2.4.2 | Sensitive analysis

In order to determine the sensitive parameters in the Kynp, the extended Fourier amplitude sensitivity test (EFAST) was employed. The total variance $\mathrm{Var}(Y)$ was acquired as following:

$$\mathrm{Var}(Y) = \sum_i V_i + \sum_{i\neq j} V_{ij} + \sum_{i\neq j\neq m} V_{ijm} + \ldots + \sum_{i\neq j\neq m\neq \ldots \neq k} V_{ijm\ldots k} \quad (2)$$

where V_i is the variability associated with the main effect of parameter i, and V_{ij} is the variability associated with the interaction between parameters i and j. The first-order sensitivity indexes (S_i) are derived from the decomposition of the above equation by dividing the importance measures by $\mathrm{Var}(Y)$:

$$S_i = \frac{V_i}{\mathrm{Var}(Y)} \quad (3)$$

$$S_{ij} = \frac{V_{ij}}{\mathrm{Var}(Y)} \quad (4)$$

where S_{ij} is the interactive sensitivity index between parameters i and j. Thus, based on the effects of its interaction with other parameters, the total sensitivity indexes (S_{Ti}) were given by:

$$S_{Ti} = \frac{V_i + V_{ij} + \ldots + V_{ij\ldots k}}{\mathrm{Var}(Y)} \quad (5)$$

A higher S_i or S_{Ti} indicates a higher contribution to the response variables of interest, and vice versa. S_i and S_{Ti} of thirty-five parameters in the Kynp were calculated by Matlab, and the codes are presented in Appendix S1. Based on Cannavo,[21] the sensitivity value (S_{Ti}) larger than 0.5 was defined as a sensitive parameter; otherwise, it was defined as an insensitive parameter.

2.5 | Biological analysis of sensitive and insensitive factors

In order to confirm the accuracy of sensitivity analysis calculations, experiments were performed using siRNA technique to knock down the expression of sensitive and insensitive parameters, and then TGF-β1 expression was assessed as an indicator of Kynp activity. Based on the sensitivity analysis results, three siRNA sequences were designed for sensitive and insensitive genes as listed in Table S2. The experiment was divided into three groups: siRNA group, negative control (NC) group, and normal group. For sensitive parameter evaluation, a real-time polymerase chain reaction (RT-PCR) experiment was done to test the relative mRNA expression of *TGF-β1* under the condition of knocking down *Kyn*, *GPR35*, *NF-kβp105*, and *NF-kβp65* gene expression using siRNA. For insensitive parameter evaluation, similarly, the relative expression of *TGF-β1* was tested under the condition of knocking down *β-catenin*, *IKK-β*, and *IL-6* gene expression using siRNA.

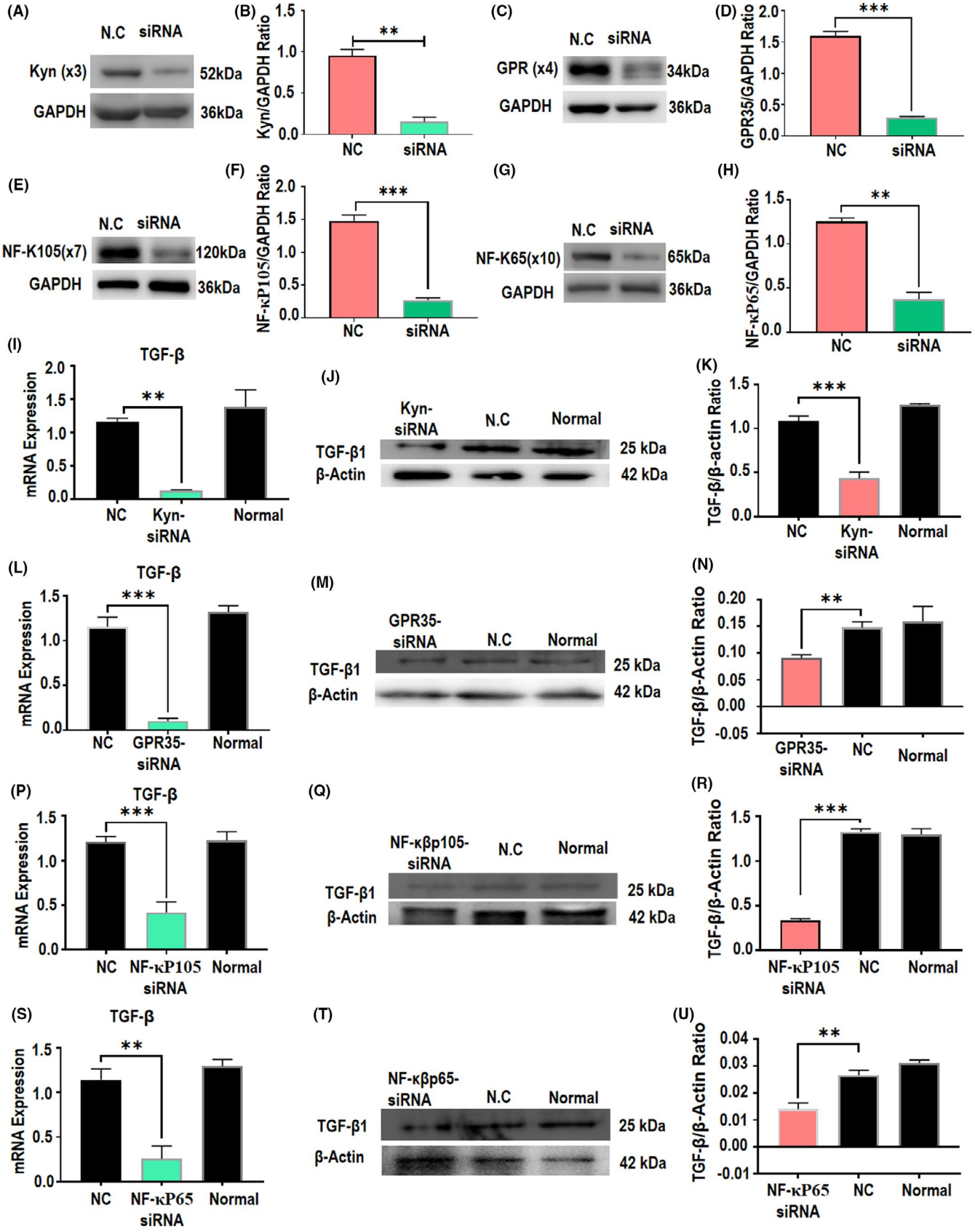
(A)
N.C siRNA
Kyn (x3) 52kDa
GAPDH 36kDa
(B)
Kyn/GAPDH Ratio
NC siRNA
(C)
N.C siRNA
GPR (x4) 34kDa
GAPDH 36kDa
(D)
GPR35/GAPDH Ratio
NC siRNA
(E)
N.C siRNA
NF-K105(x7) 120kDa
GAPDH 36kDa
(F)
NF-κP105/GAPDH Ratio
NC siRNA
(G)
N.C siRNA
NF-K65(x10) 65kDa
GAPDH 36kDa
(H)
NF-κP65/GAPDH Ratio
NC siRNA
(I)
TGF-β
mRNA Expression
NC Kyn-siRNA Normal
(J)
Kyn-siRNA N.C Normal
TGF-β1 25 kDa
β-Actin 42 kDa
(K)
TGF-β/β-actin Ratio
NC Kyn-siRNA Normal
(L)
TGF-β
mRNA Expression
NC GPR35-siRNA Normal
(M)
GPR35-siRNA N.C Normal
TGF-β1 25 kDa
β-Actin 42 kDa
(N)
TGF-β/β-Actin Ratio
GPR35-siRNA NC Normal
(P)
TGF-β
mRNA Expression
NC NF-κP105 siRNA Normal
(Q)
NF-κβp105-siRNA N.C Normal
TGF-β1 25 kDa
β-Actin 42 kDa
(R)
TGF-β/β-Actin Ratio
NF-κP105 siRNA NC Normal
(S)
TGF-β
mRNA Expression
NC NF-κP65 siRNA Normal
(T)
NF-κβp65-siRNA N.C Normal
TGF-β1 25 kDa
β-Actin 42 kDa
(U)
TGF-β/β-Actin Ratio
NF-κP65 siRNA NC Normal

FIGURE 4 The biological activity of sensitive parameters of the Kynp in the pancreatic adenocarcinoma (PDAC) cell line was confirmed at mRNA and protein expression levels. Three different siRNAs were designed to test the most effective siRNA for the gene knocking down of calculated sensitive parameters in the Kynp in Panc-1. A-B, Protein expression of the knocked down Kyn gene in the Panc-1 cell line. C-D, Protein expression of the knocked down GPR35 gene in the Panc-1 cell line. E-F, Protein expression of the knocked down NF-kβp105 gene in the Panc-1 cell line. G-H, Protein expression of the knocked down NF-kβp65 gene in the Panc-1 cell line. I, L, P, S The effect of the knockdown of *Kyn*, *GPR35*, *NF-kβp105*, and *NF-kβp65*, respectively, on the expression of TGF-β1 in the Panc-1 cell line: It showed significant reduction in the expression of *TGF-β1*. J, M, Q, T, Protein expression level of TGF-β1 in the case of kyn, *GPR35*, *NF-kβp105*, and *NF-kβp65* knockdown, respectively. K, N, R, U, Normalized ratio of *TGF-β1* expression in the case of kyn, *GPR35*, *NF-kβp105*, or *NF-kβp65* knockdown, respectively (error bars, mean ± SD; **P* < .05, ***P* < .01, ****P* < .001, *****P* < .0001, Tukey's post hoc test)

Panc-1 cell line was cultured in a 48-well plate in DMEM without antibiotic for 24 hours. Next, cells were transfected by siRNA using the protocol of lipofectamine-2000 (Thermo Fisher). Later, cells were incubated for 18 hours and then washed, collected, and used for extracting total RNA. The primers listed in Table S1 were used to assess target gene expression. Effective siRNAs have been selected for sensitive analysis test. Kynureninase has been targeted by Kyn-siRNA, GPR35R by GPR35-siRNA, NF-κβp105 by NF-κβp105-siRNA, and NF-κβp65 by NF-κβp65-siRNA. Thereafter, transfected cells were collected, washed, and used to test TGF-β1 expression by RT-PCR and Western blot using the same protocol as described above. Moreover, insensitive parameters (β-catenin, IKK-β, and IL-6) were assessed by the same method as the one used for sensitive parameters using β-catenin-siRNA, IKK-β-siRNA, and IL-6-siRNA, respectively.

2.6 | Statistical analysis

All data were presented as the mean ± SD. Differences between the values were evaluated using one-way analysis of variance (Tukey's post hoc test), except in vivo biocompatibility experiment (Tukey's post hoc test). Data were presented as means with 95% confidence interval. $P < .05$ was considered statistically significant.

3 | RESULTS

3.1 | Mathematical model of the Kynp was successfully established based on mRNA expression trends of Kynp molecules

Relative mRNA expression of nine consecutive molecules in the Kynp was assessed for 72 hours, in 6-hour intervals, as seen in Figure 1A-I and Table S1. The expression of the tested molecules showed obvious changes under the effect of IDO1 in a time-dependent manner. It showed significant increase from 6 hours to 72 hours that enhanced the increase of TGF-β1 in the Panc-1 cell line. Based on the relative mRNA expression, thirty-five parameters were estimated by the *fmincon* function and *lsqnonlin* function (Matlab 2017b) to establish the model according to expression trends (see the list in Data S1). The model was validated by plotting the experimental findings (red line) and model simulations (blue line) as shown in Figure 1J-U. We noticed that experimental findings and model stimulation were well fitted. The correlation coefficient (R) was computed between experimental findings and model stimulation. Results as shown in Table S4 illustrated that the R value of all tested variables displayed strong correlations ($R > 0.988$) suggesting that the model is efficient.

Moreover, in order to test the accuracy and predictability of the model, further experiments were performed at time points 10 hours, 20 hours, 40 hours, and 80 hours, as shown in Figure 2A-I and Figure S1A-I. The expression of Kynp molecules confirmed the significant upward changes in a time-dependent manner. The expression trends of Kynp molecules at time points 10 hours, 20 hours, and 40 hours were used to test the accuracy of the model, while the experimental data at time point 80 hours was used to test predictability of the model. The results, as seen in Figure 2J-U, showed high accuracy of the model simulation from 0 hours to 72 hours and efficient predictability in the trends of Kynp molecule expression from 72 hours to 80 hours. Further, the calculation of R values between mathematical model simulation and experimental results showed R larger than 0.988, as seen in Table S5, which indicates the high accuracy of the established model in the prediction of the activity of Kynp molecules in PDAC.

3.2 | Protein expression trends of Kynp molecules confirmed the established model

In order to verify the mathematical model at protein expression level, ELISA and Western blot were performed. The protein expression levels of kynurenine, β-catenin, NF-κβp65, and TGF-β1 were tested for 72 hours in 6-hour intervals by ELISA kits. The results showed increased protein expression trends of kynurenine, β-catenin, NF-κβp56, and TGF-β1 from 6 hours to 72 hours, as presented in Figure 3A-D, that interestingly were in line with the genetic profiling results. Western blot analysis, as shown in Figure 3E and Figure S3A-D, presented the same increasing trend of protein expression of GPR35, β-catenin, NF-κβp105, and TGF-β1 from 6 hours to 80 hours.

3.3 | The prediction of sensitive molecules in the Kynp based on the mathematical model

The global sensitivity analysis EFAST was performed to evaluate the sensitivity of 35 parameters in the Kynp. The results, as shown in

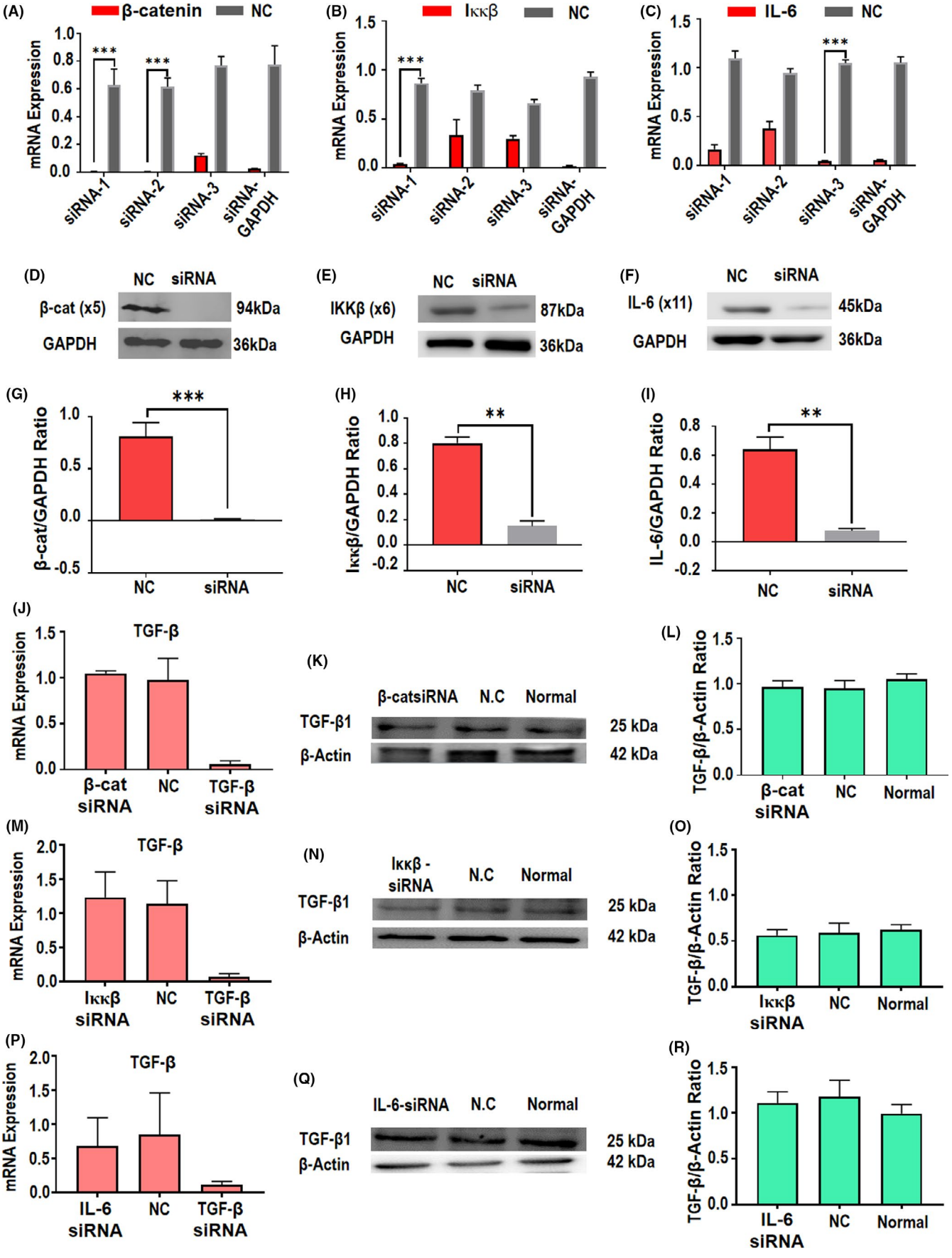
(A)
β-catenin
NC
mRNA Expression
1.0
0.8
0.6
0.4
0.2
0.0
***
***
siRNA-1
siRNA-2
siRNA-3
siRNA-GAPDH
(B)
Iκκβ
NC
mRNA Expression
1.5
1.0
0.5
0.0
***
siRNA-1
siRNA-2
siRNA-3
siRNA-GAPDH
(C)
IL-6
NC
mRNA Expression
1.5
1.0
0.5
0.0
***
siRNA-1
siRNA-2
siRNA-3
siRNA-GAPDH
(D)
NC
siRNA
β-cat (x5)
94kDa
GAPDH
36kDa
(E)
NC
siRNA
IKKβ (x6)
87kDa
GAPDH
36kDa
(F)
NC
siRNA
IL-6 (x11)
45kDa
GAPDH
36kDa
(G)
β-cat/GAPDH Ratio
1.0
0.5
0.0
-0.5
***
NC
siRNA
(H)
Iκκβ/GAPDH Ratio
1.0
0.8
0.6
0.4
0.2
0.0
-0.2
**
NC
siRNA
(I)
IL-6/GAPDH Ratio
0.8
0.6
0.4
0.2
0.0
-0.2
**
NC
siRNA
(J)
TGF-β
mRNA Expression
1.5
1.0
0.5
0.0
β-cat siRNA
NC
TGF-β siRNA
(K)
β-catsiRNA
N.C
Normal
TGF-β1
25 kDa
β-Actin
42 kDa
(L)
TGF-β/β-Actin Ratio
1.5
1.0
0.5
0.0
β-cat siRNA
NC
Normal
(M)
TGF-β
mRNA Expression
2.0
1.5
1.0
0.5
0.0
Iκκβ siRNA
NC
TGF-β siRNA
(N)
Iκκβ - siRNA
N.C
Normal
TGF-β1
25 kDa
β-Actin
42 kDa
(O)
TGF-β/β-Actin Ratio
1.5
1.0
0.5
0.0
Iκκβ siRNA
NC
Normal
(P)
TGF-β
mRNA Expression
2.0
1.5
1.0
0.5
0.0
IL-6 siRNA
NC
TGF-β siRNA
(Q)
IL-6-siRNA
N.C
Normal
TGF-β1
25 kDa
β-Actin
42 kDa
(R)
TGF-β/β-Actin Ratio
1.5
1.0
0.5
0.0
IL-6 siRNA
NC
Normal

FIGURE 5 The biological activity of insensitive parameters in the Kynp in the pancreatic adenocarcinoma (PDAC) cell line was confirmed at mRNA and protein expression levels. Three different siRNAs were designed to test the most effective siRNA for the gene knocking down of calculated insensitive parameters in the Kynp in Panc-1. A-C, Results of gene relative expression of β-catenin, Iκκβ, and IL-6, respectively, in Panc-1 under siRNA down regulation. D-I, Performance of the selected siRNA in the knocking down of every tested gene. J, M, P, the *TGF-β1* gene expression results under the effect of β-catenin, IKK-β, or IL-6 knockdown showed no statistical differences in the *TGF-β1* levels in comparison with the negative control group. K, N, Q, Protein expression levels of TGF-β1 under the effect of β-catenin, IKK-β, or IL-6 knockdown, respectively. L, O, R, Normalized TGF-β1 expression ratio according to β-Actin expression

Table 1 and Figure 3F, G, presented the sensitive and insensitive parameters in the Kynp. Sensitive parameters were defined by $S_{Ti} > 0.5$ ($a_2 = 0.6516$, $a_6 = 0.7622$, $a_8 = 0.6172$, $a_{16} = 0.5870$, $a_{18} = 0.5260$, $b_4 = 0.7760$, $b_6 = 0.5710$, $b_7 = 0.5320$, $b_8 = 0.7180$, $b_{10} = 0.6950$, and $b_{11} = 0.5240$). In order to confirm the sensitivity of the selected parameters, gene-silencing experiments were performed. However, the sensitivity of the degradation parameters (b4, b6, b7, b8, b10, b11) has been ignored because we just focused on the expression level of the activation parameters (a2, a6, a8, a16, a18). Furthermore, the IDO1 produced by cells was mixed with the added IDO1 in the culture; thus, the a2 (IDO1) experimental test was ignored because it would affect the model calculation. Therefore, a6, a8, a16, and a18 were defined as sensitive molecules in the Kynp.

3.4 | Sensitive molecules in the Kynp showed significant effect on the expression of TGF-β1

As shown in Figure 3G, parameter (a6) $S_{Ti} = 0.7622$ reflects the high sensitivity of activation rate from Kyn to GPR35. The knockdown of the *Kyn* gene, as presented in Figure 4A and B and Figure S4A, significantly reduced the expression of TGF-β1 in comparison with the negative control ($P = .0001$) at the gene expression level and protein expression level, as seen in Figure 4I, J, K. Further, the activation rate of *GPR35* to *β-catenin*, *NF-kβp105* to *ANK*, and *NF-kβp65* to *RelA* showed sensitive values (a8 = 0.6172, a16 = 0.5870, a18 = 0.5260) that were also successfully silenced using siRNA transfection as shown in Figure 4C, D and Figure S4B for *GPR35*, Figure4E, F, and Figure S4C for *NF-kβp105* as well as Figure 4G, H and Figure S4D for *NF-kβp65*. Similarly, knockdown of *GPR35*, *NF-kβp105*, and *NF-kβp65* significantly reduced the expression level of *TGF-β1* in te PDAC ($P < .0001$, $P < .0005$, $P < .0012$), respectively (gene and protein expression levels are presented in Figure 4L-N, P-R, S-U). It is also noticed that there is a negative relationship between sensitivity value and *TGF-β1* relative expression: Higher sensitivity showed a lower *TGF-β1* relative expression. Also, the comparison of the siRNA group with the normal group presented the same significant relationship between the selected sensitive parameters and *TGF-β1* relative expression (Figure 4I, L, P, S).

Furthermore, we also verified the significant relationship between sensitive parameters (a6, a8, a16, a18) and TGF-β1 protein expression in PDAC by Western blot (Figure 4J, M, Q, T). When *Kyn* was silenced, the TGF-β1 protein expression ratio was significantly reduced ($P < .01$) in comparison with the NC and normal group (0.4 ± 0.07, 1.08 ± 0.05, 1.26 ± 0.019, respectively). Moreover, the silencing of *GPR35* ($P < .01$), *NF-kβp105* ($P < .001$), and *NF-kβp65* ($P < .01$) significantly reduced the protein expression ratio of TGF-β1 in the PDAC cell line in comparison with the NC and normal group (0.090 ± 0.01, 0.147 ± 0.01, 0.16 ± 0.02; 0.33 ± 0.02, 1.32 ± 0.04, 1.3 ± 0.07; 0.135 ± 0.04, 0.27 ± 0.04, 0.3 ± 0.008; respectively). Altogether, the experimental evidence interestingly proved the high sensitivity of the calculated sensitive parameters. This evidence strongly indicated the sensitive parameters are attractive, novel therapeutic targets in the Kynp that could contribute to the treatment of PDAC.

To confirm the significant effect of sensitive parameters, insensitive parameters were also tested by qPCR and Western blot to compare their effects on TGF-β1 expression levels in the PDAC cell line. Three parameters with less than 0.5 (a7 = 0.2803, a9 = 0.2944, a19 = 0.2324) have been selected, which represent the mRNA expression level of *β-catenin*, *IKK-β*, and *IL-6* in the Kynp, respectively. The experimental analysis of these insensitive parameters showed that when *β-catenin* was knocked down, the relative expression of *TGF-β1* showed no statistical differences in comparison with the NC group ($P = .6378$). Also, knockdown of *IKK-β* or *IL-6* molecules presented no statistical differences in the expression of *TGF-β1* in the PDAC cell line ($P = .7678$ and $P = .7099$, respectively), as shown in Figure 5J, M, P. The selection of efficient siRNA and the confirmation of the downregulation of insensitive genes in PDAC are presented in Figure 5A-I. The confirmation of insensitive parameter effects was performed by Western blot that showed no significant differences in the TGF-β1 protein expression levels when *β-catenin*, *IKK-β*, or *IL-6* were silenced ($P = .2612$, $P = .6636$, and $P = .3038$, respectively), as presented in the Figure 5K-L, N-O, Q-R. This means the insensitive parameters should be ignored in the therapeutic application trials against the Kynp in PDAC. These results also confirmed the effect of sensitive parameters on the expression level of TGF-β1.

Altogether, the established model importantly showed accuracy in predicting targeted molecules in the Kynp that suggested to be considered in advanced trials of PDAC treatment.

4 | DISCUSSION

Pancreatic adenocarcinoma remains one of the highest-mortality gastrointestinal tract cancers in the world.[1] Up to date, there is no superior target to reduce PDAC mortality or improve survival rate. Conventional chemotherapy failed to provide any therapeutic improvements.[22] Current research pays much attention to Kynp triggering in pancreatic cancer using IDO inhibitors because

it presented a promising immunotherapeutic strategy against PDAC[23,24] (ClinicalTrials.gov Identifier: NCT02077881). However, the lack of sensitive targets in the Kynp is challenging in the treatment of PDAC in clinical trials.[25,26]

In this study, we have established a mathematical model for accurately calculating the activity of Kynp molecules and predicting the sensitive parameters in the Kynp in PDAC. Recent statistical and mathematical models of PDAC have considered mortality database or disease risk factors.[27,28] However, our mathematical model introduces critical informative outputs describing Kynp molecules' activity in PDAC based on ordinary differential equations, which is a type of more advanced modeling, as recently reported.[28,29] This model describes the dynamic expression trends of every parameter in the Kynp depending on concentration changes, which can not only contribute to deep understanding of Kynp activity but also forecast the trend of molecular activities and quantitatively analyze the molecular mechanisms of the Kynp regulating PDAC, as well as explore novel therapeutic targets.

By tracking the literature, twelve consecutive molecules involving the Kynp were included in the model establishment, starting with tryptophan amino acid, the main substrate of the Kynp;[30] IDO1, the main mediator of Kynp;[31] then GPR35;[32] β-catenin;[7,33] IKK-β; NF-κβ;[10,11] NF-κβp65;[12] IL-6;[13] and finally TGF-β1, the essential biomarker of the Kynp in PDAC.[14-17] The correlation efficient of these molecules has been measured by Pearson's correlation coefficient (*R*), which measures linear trends.[34] It displayed >0.988 for all selected variables, which indicated the strong relationship between the established model and the expression trends of all variables in the Kynp. Moreover, the analysis of sensitivity explored significant sensitive targets in the Kynp (kynureninase, GPR35, NF-κβp105, or NF-κβp65) that can contribute to efficiently inhibiting the Kynp in PDAC. The significant effect of sensitive parameters was confirmed by testing the opposite insensitive parameters that showed no significant effects on the activity of the Kynp in the PDAC cell line. These findings support newly published studies that describe the increase of kynurenine metabolites in the serum as a risk factor for pancreatic cancer,[35] GPR35 as a novel target in pancreatic cancer and other tumors,[36,37] and NF-κβ as the most active player in pancreatic and human cancers.[38-40] Further, our study evidenced that β-catenin is an insensitive parameter in the Kynp in PDAC, which is in contrast with a published report that suggested that kynurenine activates β-catenin to enhance breast cancer cell proliferation and metastasis.[7] These contradictory findings could be ascribed to the genetic differences of every tumor cell line. Also, although, β-catenin has no significant effect on the TGF-β1 expression levels, it could participate in cancer cell proliferation indirectly. In addition, IKKβ and IL-6 have been noticed to be insensitive in the Kynp, as they did not show a significant effect on the production of TGF-β1 in the Panc-1 cell line. Previous studies showed an unclear role of IL-6 in PDAC.[41] It could support cancer progression by playing a secondary role, which suggests a low significance of targeting the

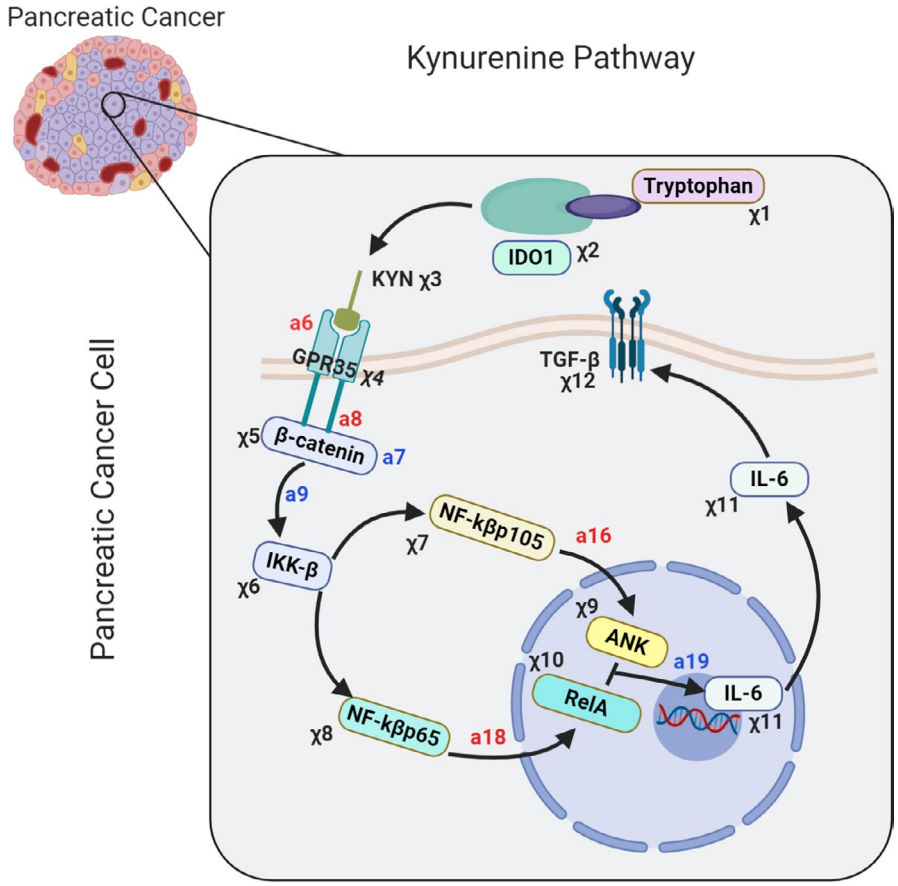

FIGURE 6 Kynurenine pathway in the pancreatic adenocarcinoma. The schematic diagram shows the production and effects of all variables in the pathway that stimulate TGF-β1 production as a marker of tumor cell survival. These variables have a production rate which is presented as X. It is an equation of predicted product during specific time. The model has been built according to the gene profiling of all variables presented in the figure

IL-6 gene. Indeed, IKKβ could participate with other genes in the rapid proteosomal degradation leading to the release of NF-κB and enhancing DNA binding, which could be mediated by other genes. Thus, the blocking of IKKβ is useless for inhibiting the activity of the Kynp in PDAC.[42] The limitations of this study can be summarized as the follows: Using one kind of pancreatic cancer cells which is one of the most virulent types could be one of the limitations. However, it could work also with other pancreatic cell types, so this point needs further investigation in the future. Further, the prediction efficiency of the mathematical model in vivo has not been tested. As in vitro evaluation of gene expression is mostly different to in vivo evaluation, in vivo experiments are required in the future for evaluating this model accurately to explore the potential for in vivo prediction efficacy.

In conclusion, the activity of Kynp molecules as shown in Figure 6 have been elucidated by a newly established mathematical model. This is supposed to contribute to tracking, predicting, and modulating the biological activity of the Kynp. It could provide a promising tool to targeting PDAC through the downregulation of sensitive parameters. In addition, the established mathematical model could be applied to other cancers considering the Kynp with appropriate modifications.

ACKNOWLEDGMENTS

This work was supported by the National Natural Science Foundation of China (No. 81972116; No. 81972085; No. 81772394); Key Program of Natural Science Foundation of Guangdong Province (No.2018B0303110003); Shenzhen Peacock Project (KQTD20170331100838136); Shenzhen Science and Technology Projects (No. JCYJ20170817172023838; No. JCYJ20170306092215436; No. JCYJ20170412150609690; JCYJ20170413161649437; No. JCYJ20170413161800287); Special Funds for the Construction of High-Level Hospitals in Guangdong Province, and International Science and Technology Cooperation Project (1035043).

CONFLICT OF INTEREST

The authors declare that they have no conflict of interest. Our institution did not receive payment or services from a third party (government, commercial, private foundation, etc.) for any aspect of the submitted work. There are no relevant financial activities outside the submitted work.

DATA AVAILABILITY STATEMENT

The authors declare that all data supporting the results of this study are available within the paper and its Appendix S1.

ORCID

Daping Wang https://orcid.org/0000-0002-2402-8134

REFERENCES

1. Simoes PK, Olson SH, Saldia A, Kurtz RC. Epidemiology of pancreatic adenocarcinoma. *Chinese Clin Oncol*. 2017;6(3):24.
2. Kalimuthu Sangeetha, Notta Faiyaz. Molecular pathogenesis of pancreatic ductal adenocarcinoma. *Diagnostic Histopathol*. 2016;22:226-235.
3. Blesl C, Tmava A, Baranyi A, et al. The Kynurenine pathway in pancreatic carcinoma. *Eur Psychiat*. 2017;41:S480.
4. Botwinick IC, Pursell L, Yu G, Cooper T, Mann JJ, Chabot JA. A biological basis for depression in pancreatic cancer. *HPB (Oxford)*. 2014;16:740-743.
5. Bishnupuri KS, Alvarado DM, Khouri A, et al. IDO1 and Kynurenine Pathway Metabolites Activate PI3K-Akt Signaling in the Neoplastic Colon Epithelium to Promote Cancer Cell Proliferation and Inhibit Apoptosis. *Can Res*. 2019;79:1138-1150.
6. Schneditz G, Elias JE, Pagano E, et al. GPR35 promotes glycolysis, proliferation, and oncogenic signaling by engaging with the sodium potassium pump. *Sci Signal*. 2019;12:eaau9048.
7. Thaker AI, Rao MS, Bishnupuri KS, et al. IDO1 metabolites activate β-catenin signaling to promote cancer cell proliferation and colon tumorigenesis in mice. *Gastroenterology*. 2013;145:416-425.
8. Alahdal M, Xing Y, Tang T, Liang J. 1-Methyl-D-tryptophan Reduces Tumor CD133(+) cells, Wnt/β-catenin and NF-κβp65 while Enhances Lymphocytes NF-κβ2, STAT3, and STAT4 Pathways in Murine Pancreatic Adenocarcinoma. *Sci Rep*. 2018;8:9869.
9. Chimge NO, Little GH, Baniwal SK, et al. RUNX1 prevents oestrogen-mediated AXIN1 suppression and β-catenin activation in ER-positive breast cancer. *Nat Commun*. 2016;7:10751.
10. Ma B, Hottiger MO. Crosstalk between Wnt/β-Catenin and NF-κB Signaling Pathway during Inflammation. *Front Immunol*. 2016;7:378.
11. Rodriguezpinilla M, Rodriguezperalto JL, Hitt R, et al. β-Catenin, Nf-κB and FAS protein expression are independent events in head and neck cancer: study of their association with clinical parameters. *Cancer Lett*. 2005;230:141-148.
12. Hemmati S, Sadeghi MA, Jafari RM, Yousefimanesh H, Dehpour AR. The antidepressant effects of GM-CSF are mediated by the reduction of TLR4/NF-κB-induced IDO expression. *J Neuroinflammation*. 2019;16:117.
13. Zhang W, Zhang J, Zhang Z, et al. Overexpression of Indoleamine 2,3-Dioxygenase 1 Promotes Epithelial-Mesenchymal Transition by Activation of the IL-6/STAT3/PD-L1 Pathway in Bladder Cancer. *Translat Oncol*. 2019;12:485-492.
14. Pelak MJ, Śnietura M, Lange D, Nikiel B, Pecka KM. The prognostic significance of indoleamine-2,3-dioxygenase and the receptors for transforming growth factor β and interferon γ in metastatic lymph nodes in malignant melanoma. *Polish J Pathol*. 2015;66:376-382.
15. Mbongue JC, Nicholas DA, Torrez TW, Kim N, Firek A, Langridge WHR. The Role of Indoleamine 2, 3-Dioxygenase in Immune Suppression and Autoimmunity. *Vaccine*. 2015;3:703-729.
16. Belladonna ML, Orabona C, Grohmann U, Puccetti P. TGF-β and kynurenines as the key to infectious tolerance. *Trends Mol Med*. 2009;15:41-49.
17. Javle M, Li Y, Tan D, et al. Biomarkers of TGF-β Signaling Pathway and Prognosis of Pancreatic Cancer. *PLoS One*. 2014;9(1):e85942.
18. Montévil M, Speroni L, Sonnenschein C, Soto AM. Modeling mammary organogenesis from biological first principles: Cells and their physical constraints. *Prog Biophys Mol Biol*. 2016;122:58-69.
19. Dubois G. *Modeling and Simulation*, 1st edn. Boca Raton: Taylor & Francis, CRC Press; 2018:166.
20. Tang T, Yang Z, Zhu Q, et al. Up-regulation of miR-210 induced by a hypoxic microenvironment promotes breast cancer stem cell metastasis, proliferation, and self-renewal by targeting E-cadherin. *FASEB J*. 2018;32:6965-6981.
21. Cannavo F. Sensitivity analysis for volcanic source modeling quality assessment and model selection. *Comput Geosci*. 2012;44:52-59.
22. Wang J, Chai J, Liu L, et al. Dual-functional melanin-based nanoliposomes for combined chemotherapy and photothermal therapy of pancreatic cancer. *RSC Advances*. 2019;9:3012-3019.

23. Blair AB, Kleponis J, Thomas DL, et al. IDO1 inhibition potentiates vaccine-induced immunity against pancreatic adenocarcinoma. *J Clin Investig*. 2019;129:1742-1755.
24. Liu M, Wang X, Wang L, et al. Targeting the IDO1 pathway in cancer: from bench to bedside. *J Hematol Oncol*. 2018;11:100.
25. Hu ZI, Hellmann MD, Wolchok JD, et al. Acquired resistance to immunotherapy in MMR-D pancreatic cancer. *J Immuno Therap Can*. 2018;6:127.
26. Prendergast GC, Malachowski WP, Duhadaway JB, Muller AJ. Discovery of IDO1 Inhibitors: From Bench to Bedside. *Can Res*. 2017;77:6795-6811.
27. Hanada K, Amano H, Abe T. Early diagnosis of pancreatic cancer: Current trends and concerns. *Ann Gastroenterol Surg*. 2017;1:44-51.
28. Kalamakis G, Brune D, Ravichandran S, et al. Quiescence Modulates Stem Cell Maintenance and Regenerative Capacity in the Aging Brain. *Cell*. 2019;176(6):1407-1419.
29. Li Y, Yi M, Zou X. The linear interplay of intrinsic and extrinsic noises ensures a high accuracy of cell fate selection in budding yeast. *Sci Rep*. 2014;4:5764.
30. Cervenka I, Agudelo LZ, Ruas JL. Kynurenines: Tryptophan's metabolites in exercise, inflammation, and mental health. *Science*. 2017;357(6349):eaaf9794.
31. Bilir C, Sarisozen C. Indoleamine 2,3-dioxygenase (IDO): Only an enzyme or a checkpoint controller? *J Oncol Sci*. 2017;3:52-56.
32. Agudelo LZ, Ferreira DMS, Cervenka I, et al. Kynurenic Acid and Gpr35 Regulate Adipose Tissue Energy Homeostasis and Inflammation. *Cell Metab*. 2018;27(2):378-392.
33. Wirthgen E, Hoeflich A, Rebl A, Gunther J. Kynurenic Acid: The janus-faced role of an immunomodulatory tryptophan metabolite and its link to pathological conditions. *Front Immunol*. 2018;8(1957). https://doi.org/10.3389/fimmu.2017.01957.
34. Altman N, Krzywinski M. Association, correlation and causation. *Nat Methods*. 2015;12:899-900.
35. Huang JY, Butler LM, Midttun Ø, et al. A prospective evaluation of serum kynurenine metabolites and risk of pancreatic cancer. *PLoS One*. 2018;13:e0196465.
36. Shore DM, Reggio PH. The therapeutic potential of orphan GPCRs, GPR35 and GPR55. *Front Pharmacol*. 2015;6:69.
37. Mackenzie AE, Lappin JE, Taylor DL, Nicklin SA, Milligan G. GPR35 as a Novel Therapeutic Target. *Front Endocrinol (Lausanne)*. 2011;2:68.
38. Wang L, Zhou W, Zhong Y, et al. Overexpression of G protein-coupled receptor GPR87 promotes pancreatic cancer aggressiveness and activates NF-κB signaling pathway. *Mol Cancer*. 2017;16:61.
39. Xia Y, Shen S, Verma IM. NF-κB, an active player in human cancers. *Cancer Immunol Res*. 2014;2:823-830.
40. Rimmon A, Vexler A, Berkovich L, Earon G, Ron I, Levari S. Escin Chemosensitizes Human Pancreatic Cancer Cells and Inhibits the Nuclear Factor-kappaB Signaling Pathway. *Biochem Res Int*. 2013;2013:251752.
41. Pop V-V, Seicean A, Lupan I, Samasca G, Burz C-C. IL-6 roles – Molecular pathway and clinical implication in pancreatic cancer – A systemic review. *Immunol Lett*. 2017;181:45-50.
42. Wu D-G, Yu P, Li J-W, et al. Apigenin potentiates the growth inhibitory effects by IKK-β-mediated NF-κB activation in pancreatic cancer cells. *Toxicol Lett*. 2014;224:157-164.

SUPPORTING INFORMATION

Additional supporting information may be found online in the Supporting Information section.

How to cite this article: Alahdal M, Sun D, Duan L, et al. Forecasting sensitive targets of the kynurenine pathway in pancreatic adenocarcinoma using mathematical modeling. *Cancer Sci*. 2021;112:1481–1494. https://doi.org/10.1111/cas.14832